Iranian Journal of Chemical Engineering
Vol. 2, No. 2, 2005, IAChE

Reactor Modeling of a Non-Catalytic OCM Process

*M. Kazemeini[*1] and A.R. Mohammadi[**2]*
1. Department of Chemical & Petroleum Engineering, Sharif University of Technology,Tehran, Iran.
2. Project Engineering Division of National Iranian Petrochemical Company, Tehran, Iran.

Abstract
One method for conversion of methane to more valuable products is by non-catalytic gas-phase oxidative coupling of methane (OCM), through which methane is converted into ethylene. The product of this process is ethylene, accompanied by acetylene, ethane, a small quantity of three carbon compounds as coupling products, and carbon oxides due to complete oxidation of hydrocarbons. The kinetic model proposed for the OCM process consists of 75 elementary reactions and 23 chemical species. In previous studies, the reactor-kinetic modeling of this process, was implemented in a laboratory micro-reactor at constant temperature and pressure. Considering that this process proceeds with severe variation in the enthalpy, in the present study, in addition to isothermal, the operation of the system has also been modeled for the adiabatic state. The modeling has been carried out in a tubular reactor system. Comparison of the qualitative and quantitative results of the model with experimental data at constant temperature shows that the proposed kinetic model predicts the experimental results properly. Furthermore, in the present study, the effect of various parameters on the operation of the system has also been examined. These studies have been performed in the following ranges of pressure, temperature and CH_4/O_2 ratio respectively: $1 \leq P \leq 10$ (bar), $950 \leq T \leq 1100$ (K), $4 \leq CH_4/O_2 \leq 10$. It has been shown that, by increasing the temperature, the reaction rate increases. Raising the total pressure of the system causes an increase in methane conversion and selectivities of desired products as well as the reaction rate. On the other hand, increasing the residence time in the reactor will result in conversion of desired products to undesirable ones. Finally, it is shown that by decreasing the ratio of methane to inlet oxygen, conversion of methane increases, selectivities of the desired products decrease and the heat released during the reaction rises.

Introduction
Following the oil crisis of the 1970s, industrially developed countries, as the major consumers of fossil fuels, made a widespread effort to replace petroleum by synthetic fuels (synfuels). For this purpose, extensive research was carried out on utilizing natural gas as a cheap and abundant chemical source. Despite the fact that the I. R. of Iran owns about 15 percent of the total natural gas reservoirs of the world, its share of the annual production of natural gas is only 1.3 percent [1]. Therefore, natural gas may be supplied in abundance and with low price as a primary feed for plants designed to convert methane into more valuable products. This fact plays a key role in justifying research, concerning conversion of methane to more

* - E-mail: kazemini@sharif.edu
** - E-mail: ar-mohammadi@nipc.net

valuable products.
The major constituent of natural gas is methane. Thus, liquefaction of the former is very difficult and un-economic. Therefore, production of more valuable products from methane can only be accomplished through chemical reactions.
Due to its rather low free Gibbs energy, methane is thermodynamically a very stable substance; thus, the reaction of production of less stable hydrocarbons from methane is limited by thermodynamical equilibrium requiring too much energy.
OCM is one of the direct processes for methane conversion to more valuable products, and has been the subject of widespread research in recent years. This process is usually performed catalytically; however, latterly research has shown that the process may also be carried out non-catalytically, yielding products similar to those of the catalytic process. The rate, selectivity and operational conditions of the non-catalytic process are somewhat different from those of the catalytic one.
Generally in the OCM process, production of methyl radicals is the controlling step of the reaction rate [2,3]. In the catalytic process, methyl radicals are produced on the catalyst; but in the gas-phase, the production of these species is facilitated by reaction of methane and oxygen. Gas phase OCM, requires oxygen in the feed to produce methyl radicals.
The reactor-kinetic model of the gas phase OCM process has been performed by several researchers [4-9], all of whom used a laboratory tubular micro-reactor at constant temperature. In addition, various kinetic models have been proposed, the basis of which was the kinetic data of elementary reactions involved in combustion [10,11]. It is worth mentioning that this process is highly exothermic and therefore, during the reaction process, the temperature will in-crease and subsequently, the rate and selecti-vity of the products will be severely affected. Calculation of the reaction heat and tem-perature variation along the length of the reactor is possible by using an adiabatic modeling procedure.
Studying the gas-phase OCM process is important from two viewpoints:

a. ***As a part of the catalytic OCM process:*** The catalyst in the OCM process plays the role of activating methane, resulting in production of a considerable amount of methyl radical as initiator of branched chain reactions in the gas phase.

b. ***As an independent process:*** By changing the operational conditions of the gas phase, especially increasing pressure within the medium range, products similar to those of the catalytic OCM may result. Consequent-ly, in this process, all reactions including the methyl radical formation take place in the gas phase.

In this research, a reactor-kinetic model is simulated in the gas phase (i.e. non-catalytic) OCM for isothermal, as well as, adiabatic operation conditions. The former is used to experimentally verify the model and the latter is a new development, presented for the first time in this work.

Kinetics of Non-Catalytic Gas Phase OCM Process

The reactions of the gas-phase OCM process take place according to a radical mechanism consisting of a large number of elementary reactions. By studying the proposed kinetic models for the non-catalytic process, a kinetic scheme consisting of 75 elementary reaction and 23 chemical species has been presented. This is used for modeling reaction kinetics at low to medium pressure ranges. The following species are treated: H2O, H2, H2O2, CH4, O2, CH2O, CO, CO2, C2H2, C2H4, C2H6, C3H6 and C3H8; and the radicals involved are taken to be: H, O, OH, HO2, CH3, C2H3, C2H5, C3H7, COH and CH3O.
The kinetic model is presented in table 1. In this model, non-homogenous reactions such as radical termination reactions on the reactor

wall have not been taken into account since their rate is controlled by diffusion of radicals through the bulk of gas to the reactor wall. Therefore the rate of termination reactions is almost equal to the diffusion rate of the radicals, which, as compared to the rate of homogenous end reactions (i.e. gas phase), is very slow and hence considered negligible.
Considering the kinetic model presented in table 1, reactions may be classified as follows:

a. Initial stage: reactions 1 and 2.
b. Production of methyl radical: reactions 3-6, where one radical receives one hydrogen atom from the methane molecule and a methyl radical is produced.
c. Oxidation of methyl radicals to the CH2O and CH3O species: reactions 7-10.
d. Coupling of the methyl radicals to produce C2 compounds: reactions 11-13.
e. Oxidation of CH2O and CH3O to CO and CO2 species: reactions 14-27.
f. Dehydrogenation of ethane to ethylene, and ethylene to acetylene: reactions 28-32, 34-41, 43, 44, 46-48 and 50.
g. Decomposition of ethylene, acetylene and ethyl radical: reactions 33, 42, 45, 49, 51and 52.
h. Production of C3 compounds: reactions 53-59.
i. Hydrogen-Oxygen reactions: reactions 60-75.

For calculation of the rate constants of forward reactions, the well-known Arrhenius expression with the following form has been used:

$$k_{fi} = A_i T^{\beta_i} \exp\left[\frac{-E_{act,i}}{RT}\right] \qquad (1)$$

The rate constants for the reverse reactions are calculated from the following equation:

$$k_{ri} = \frac{k_{fi}}{\exp\left[\frac{\Delta S_i^0}{R} - \frac{\Delta H_i^0}{RT}\right]\left[\frac{P_{atm}}{RT}\right]^{\sum_{k=1}^{k} \nu_{ki}}} \qquad \nu_{ki} = \nu''_{ki} - \nu'_{ki} \qquad (2)$$

The values related to changes in enthalpy; entropy and heat capacity are expressed as a polynomial function[12].
In order for some reactions to occur, it is necessary that a third species also participates in them. In such reactions all species existing in the system act as a third body. These species have different effects and a term related to the effect of the third body should be inserted in the equation of the reaction rate. In the present kinetic model, reactions 11, 14, 22, 27, 35, 47, 61, 68, 69 and 75 are those in which the third bodies are accounted for in the reactions [12].

The Reactor Model

Since the intermediate products of the OCM process are the desired products, a system with minimum mixing will have a maximum efficiency. Therefore, a tubular reactor with a high length to diameter ratio will have a low dispersion number (D/UL), such that one may assume an ideal plug flow pattern inside it. In such systems, where the surface to volume ratio is high, more heat transfer surface is available. In the present research, the reactor-kinetic simulation has been performed for the isothermal and adiabatic states. Modeling under constant temperature and pressure, only the continuity equation related to the existing species in the system has been utilized, the general form of which is as follows [14]:

$$\frac{dF_k}{dV} = r_k = \sum_{i=1}^{I} r_{ik} = f_{n_k}\left(C_{T_0}\frac{F_1}{F_t}\frac{P}{P_0}\ ,\cdots,C_{T_0}\frac{F_k}{F_T}\frac{P}{P_0}\right) \qquad (3)$$

Thus K interrelated differential equations for the ***isothermal state*** have to be solved simultaneously for the adiabatic modeling,

Table 1. Proposed kinetic model for non-catalytic (gas phase) OCM

	Reaction No.	A_i	ß	E_{act}
1	$CH_4 = CH_3 + H$	3.70E15	0.00	103726
2	$CH_4 + O_2 = CH_3 + HO_2$	9.83E12	0.00	46313
3	$CH_4 + H = CH_3 + H_2$	2.34E14	0.00	12224
4	$CH_4 + O = CH_3 + OH$	1.27E15	0.00	8081
5	$CH_4 + OH = CH_3 + H_2O$	4.00E14	0.00	9897
6	$CH_4 + HO_2 = CH_3 + H_2O_2$	8.00E13	0.00	23796
7	$CH_3 + O_2 = CH_3O + O$	3.08E14	0.00	33684
8	$CH_3 + O_2 = CH_2O + OH$	4.59E13	0.00	24764
9	$CH_3 + HO_2 = CH_3O + OH$	9.00E13	0.00	0.000
10	$CH_3 + OH = CH_3O + H$	2.00E16	0.00	27473
11	$CH_3 + CH_3 + M = C_2H_6 + M$	3.65E17	0.00	0.000
12	$CH_3 + CH_3 = C_2H_5 + H$	2.40E15	0.00	26600
13	$CH_3 + CH_3 = C_2H_5 + H$	2.40E15	0.00	26600
14	$CH_3O + M = CH_2O + H + M$	2.58E20	0.00	27473
15	$CH_3O + O_2 = CH_2O + HO_2$	6.60E10	0.00	2604
16	$CH_2O + OH = CHO + H_2O$	5.80E14	0.00	1194
17	$CH_2O + HO_2 = CHO + H_2O_2$	4.17E12	0.00	9584
18	$CH_2O + O_2 = CHO + HO_2$	2.00E13	0.00	38940
19	$CH_2O + O = CHO + OH$	3.50E13	0.00	3510
20	$CH_2O + CH_3 = CHO + CH_4$	7.00E13	0.00	5979
21	$CH_2O + H = CHO + H_2$	2.50E13	0.00	3989
22	$CHO + M = CO + H + M$	2.80E15	0.00	15375
23	$CHO + O_2 = CO + HO_2$	1.71E12	0.00	0.000
24	$CHO + CH_3 = CO + CH_4$	1.20E14	0.00	0.000
25	$CO + HO_2 = CO_2 + OH$	4.50E14	0.00	25643
26	$CO + O_2 = CO_2 + O$	2.50E12	0.00	52558
27	$CO + O + M = CO_2 + M$	6.20E14	0.00	3010
28	$C_2H_6 + H = C_2H_5 + H_2$	9.10E14	0.00	12351
29	$C_2H_6 + OH = C_2H_5 + H_2O$	4.55E14	0.00	4089
30	$C_2H_6 + CH_3 = C_2H_5 + CH_4$	2.25E13	0.00	15425
31	$C_2H_6 + O_2 = C_2H_5 + HO_2$	4.00E13	0.00	50885
32	$C_2H_6 + HO_2 = C_2H_5 + H_2O_2$	2.40E13	0.00	14931
33	$C_2H_5 + HO_2 = CH_3 + CH_2O + OH$	3.00E11	0.00	0.000
34	$C_2H_5 + OH = C_2H_6 + O$	3.00E11	0.00	5972
35	$C_2H_5 + M = C_2H_4 + H + M$	5.96E19	0.00	40053
36	$C_2H_5 + O_2 = C_2H_4 + HO_2$	6.35E12	0.00	12709
37	$C_2H_5 + CH_2O = C_2H_6 + CHO$	5.50E03	2.81	5853
38	$C_2H_5 + CHO = C_2H_6 + CO$	1.20E14	0.00	0.000
39	$C_2H_4 + O_2 = C_2H_3 + HO_2$	2.81E12	0.00	34532
40	$C_2H_4 + H = C_2H_3 + H_2$	1.50E14	0.00	10201
41	$C_2H_4 + O = C_2H_3 + OH$	1.30E11	0.63	1361
42	$C_2H_4 + O = CH_3 + CHO$	1.32E08	1.55	430
43	$C_2H_4 + OH = C_2H_3 + H_2O$	6.12E13	0.00	5900
44	$C_2H_4 + CH_3 = C_2H_3 + CH_4$	1.99E11	0.00	12293
45	$C_2H_4 + OH = CH_3 + CH_2O$	2.00E12	0.00	0.000

	Reaction No.	A_i	ß	E_{act}
46	$C_2H_3 + C_2H_6 = C_2H_4 + C_2H_5$	6.00E02	3.30	10487
47	$C_2H_3 + M = C_2H_2 + H + M$	1.21E21	0.00	42151
48	$C_2H_3 + O_2 = C_2H_2 + HO_2$	5.00E12	0.00	0.000
49	$C_2H_3 + O_2 = CH_2O + CHO$	5.00E12	0.00	0.000
50	$C_2H_3 + CH_2O = C_2H_4 + CHO$	5.40E03	2.81	5853
51	$C_2H_3 + HO_2 = CH_3 + CO + OH$	3.00E13	0.00	0.000
52	$C_2H_2 + O_2 = CHO + CHO$	4.00E12	0.00	27951
53	$C_2H_5 + CH_3 = C_3H_8$	8.00E12	0.00	0.000
54	$C_2H_4 + CH_3 = C_3H_7$	1.00E11	0.00	6928
55	$C_3H_8 + H = C_3H_7 + H_2$	9.00E14	0.00	7644
56	$C_3H_8 + O = C_3H_7 + OH$	3.00E13	0.00	5757
57	$C_3H_7 + H = C_3H_8$	2.00E13	0.00	0.000
58	$C_3H_7 + HO_2 = C_3H_8 + O_2$	1.00E13	0.00	0.000
59	$C_3H_7 = C_3H_6 + H$	8.00E13	0.00	38940
60	$O_2 + H = OH + O$	2.20E14	0.00	16794
61	$O_2 + H + M = HO_2 + M$	1.40E17	0.00	0.000
62	$O + HO_2 = O_2 + OH$	2.00E13	0.00	0.000
63	$O + H_2 = OH + H$	1.50E07	2.00	7549
64	$O + H_2O = OH + OH$	4.60E09	1.31	17081
65	$O + H_2O_2 = OH + HO_2$	6.31E12	0.00	4957
66	$HO_2 + HO_2 = O_2 + OH + OH$	2.00E12	0.00	0.000
67	$OH + H_2 = H_2O + H$	1.00E08	1.60	3296
68	$H_2O_2 + M = OH + OH + M$	1.27E17	0.00	47627
69	$OH + H + M = H_2O + M$	2.20E22	-2.00	0.000
70	$OH + HO_2 = H_2O + O_2$	2.00E13	0.00	0.000
71	$OH + H_2O_2 = H_2O + HO_2$	1.75E12	0.00	0.317
72	$HO_2 + H = O_2 + H_2$	2.50E13	0.00	692
73	$HO_2 + H_2 = H_2O_2 + H$	3.00E13	0.00	26040
74	$H_2O_2 + H = OH + H_2O$	1.00E13	0.00	3965
75	$H + H + M = H_2 + M$	1.80E18	-1.00	0.000

however, the material and energy balance equations should also be taken into account such that, in addition to changes in molar rates of species along the reactor, changes in temperature and heat of reaction have to be calculated.

The following equation calculates the changes of molar flow rates throughout the reactor length for each species [14]:

$$\frac{dF_k}{dV} = r_k = \sum_{i=1}^{I} r_{ik} = fn_k\left(C_{T0}\frac{F_1}{F_t}\frac{P}{P_0}\frac{T}{T_0},\cdots,C_{T0}\frac{F_k}{F_T}\frac{P}{P_0}\frac{T}{T_0}\right) \quad (4)$$

while temperature gradients along the reactor, are calculated from the following equation [14]:

$$\frac{dT}{dy} = \frac{A\sum_{k=1}^{K} H_k \sum_{i=1}^{I} r_{ik}}{\sum_{k=1}^{K} F_k C_{pk}} \quad (5)$$

Furthermore the pressure change due to momentum losses along the reactor is calculated from the following equation [14]:

$$\frac{dP}{dy} = \frac{PG^2}{(G^2 - P\rho)}\left[\frac{\overline{W}}{G}\sum_{k=1}^{K}\omega_k + \frac{1}{T}\frac{dT}{dy} + \frac{2f}{D}\right] \quad (6)$$

In the ***adiabatic state***, consequently there are K+2 interrelated differential equations, needed to be solved simultaneously. These equations are first order stiff type differential equations, and the variable step size method applied to solve them.

Ultimately, the terms of reactants conversion and product selectivity are utilized in order to study the operation and efficiency of the system as follows [14]:

$$X = \frac{F_{k,0} - F_k}{F_{k,0}} \quad (7)$$

$$S_{k,CH_4} = \frac{n_c(F_k - F_{k,0})}{F_{CH_4,0} - F_{CH_4}} \quad (8)$$

In determining the friction factor coefficient along a tubular reactor length, the Darcy rational relation for compressible fluids and the Moody diagram technique[13] are utilized (operating conditions T=1078 K, P= 4 Bara and W=18 g/mol).

With obtained data, the Reynolds number for the gas flow inside the reactor is found to be 16740 [12]. As such, it is concluded to have a turbulent gas flow all through the reactor. Furthermore, it is assumed that reactor material is of commercial steel. Consequently, for a reactor of diameter 2 inches (5.08 cm), the friction factor is determined to be 0.02. For other operational conditions , involving turbulent flow inside a tube (of known material and dimensions) one may utilize this type of friction factor determination as the friction factor is known to be independent of the Reynolds number. In fact, this was the method used for cases investigated in this research.

Numerical technique used to solve equations in the model

The Backward Difference Formulas (BDF) method is the most common numerical technique used to solve the stiff first order differential equations with which we were partly faced in this investigation. When the step size, h, is fixed, the Finite Difference method is utilized, the BDF takes up the j^{th} order (i.e.; BFDj) for step (t_n, x_n) to (t_{n+1}, x_{n+1}) which is of the following form:

$$\sum_{m=1}^{j}\frac{1}{m}\nabla^m x_{n+1} - hF(t_{n+1}, x_{n+1}) = 0 \quad (9)$$

Here the algebraic equation for x_{n+1} is solved through the Newton iteration technique, for which the iteration starts at:

$$x_{n+1}^{(0)} = \sum_{m=0}^{j}\nabla^m x_n \quad (10)$$

The error generated from the BDFj, in this case, is accurately estimated using the following term:

$$\frac{1}{j+1}h^{j+1}x^{(j+1)} \approx \frac{1}{j+1}\nabla^{j+1}x_{n+1} \quad (11)$$

Therefore, the BDF technique with fixed step size is utilized for solving differential equations until the stiff behavior of these relations becomes evident. At this point a variable step size with changing order of BDF is implemented. In order to increase the stability in the stiff system of equations we are confronted with, Reiher and Klopfestein's Numerical Differential Formula (NFD) with careful selection of parameters was im-plemented. [12] As such, for very small step sizes, the second order NDF may be as precise as a second order BDF (i.e. BDF2) with h being 26% higher in the former case. Furthermore, the performance of the step size variation through the NDF in the MATLAB environment used in this investigation is desirable due to effective and

compact organization of its algorithm structure. The details of these techniques and chosen parameters are provided in reference [12].

Results of Modeling

In this section, the effect of various parameters on the operation of the system under isothermal and adiabatic conditions are discussed. Modeling results are first pre-sented for isothermal state and later those for adiabatic condition are displayed.

a. The Performance of the System at Isothermal State

Figure 1 shows how increasing the system operation temperature increases the methane conversion, as well as the selectivity of desired products. This is due to the fact that increasing the system temperature provides the required energy to break the C-H bond resulting in the formation of methyl radicals. This step is rate-determining for the process.

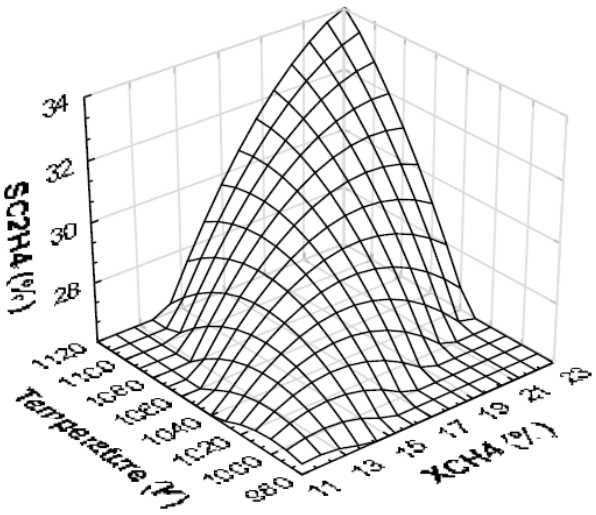

Figure 1. Effect of temperature on the amount of methane conversion and ethylene selectivity. P = 4 bar, eq = 6 , τ = 0.6 sec (Isothermal cond.)

Figure 2 shows how decreasing the ratio of methane to oxygen (eq), results in increasing the reaction rate and the amount of methane conversion. This decrease also increases the ratio of inlet oxygen, favoring complete oxidation reactions and the enhanced formation of undesired products.

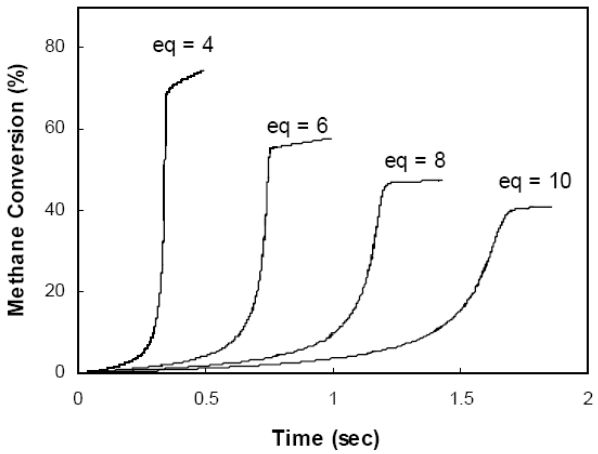

Figure 2. Effect of eq on the rate and amount of methane conversion. P = 4 bar, T = 950 K (Isothermal cond.)

Increasing the total pressure of the system causes the concentration of the reactants in the gas-phase to increase, therefore, the rate of reactions and amount of methane conversion are also increased (Figure 3). Further-more, by increasing the total pressure of the system, the production of methyl radicals and the selectivities of desired products also increase (Figure 4), while those of undesi-rable ones is lowered (Figure 5).

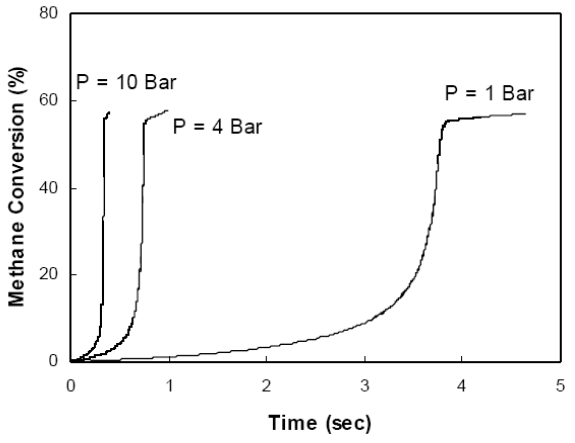

Figure 3. Effect of Total pressure on the rate and amount of methane conversion. T = 950 K, eq = 6, P= 4 bar (Isothermal cond.)

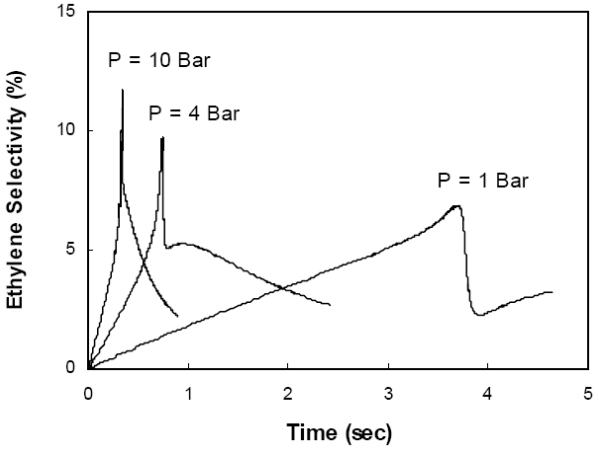

Figure 4. Effect of Total pressure on the selectivity of desired product. T = 950 K, eq = 6, P = 4 bar (Isothermal cond.)

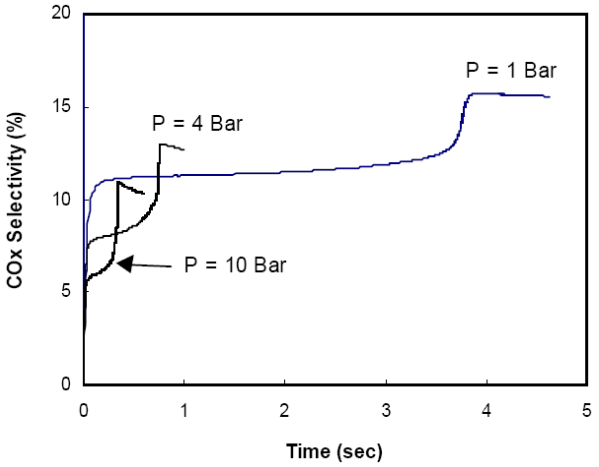

Figure 5. Effect of Total pressure on the selectivity of undesired product. T = 950 K, eq = 6, P = 4 bar (Isothermal cond.)

Figure 6 shows the changes of molar flow rate of C_2 compounds, along the reactor. The figure indicates the sequence of product formation; consisting of ethane, ethyl radical, ethylene, and acetylene.

Figure 7 shows the changes of molar flow rate of radicals in a logarithmic scale. It is apparent that methyl and hydroxyl radicals are predominant.

In Figures. 8, 9 and 10 the experimental results of Chen [9] and the results of the present model are compared. Comparison of quan-titative and qualitative results in the constanttemperature case indicate good agree-ement between the modeling and experi-mental results.

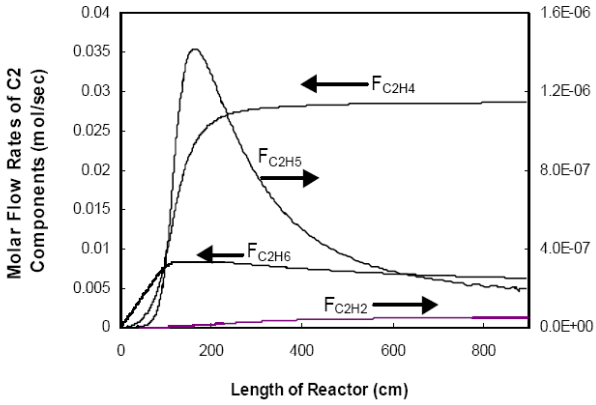

Figure 6. Changes of molar flow rate of C2 compounds along the reactor. T = 1100 K, eq = 5, P = 4 bar , $F_{CH4,0}$ = 0.85 mol/sec (Isothermal cond.)

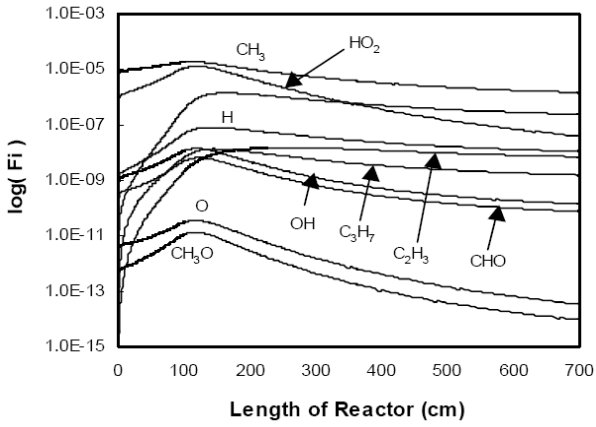

Figure 7. Changes of molar flow rate of radicals in a logarithmic scale along the reactor. T =1100 K, eq =5, P = 4 bar , $F_{CH4,0}$ = 0.85 mol/sec (Isothermal cond.)

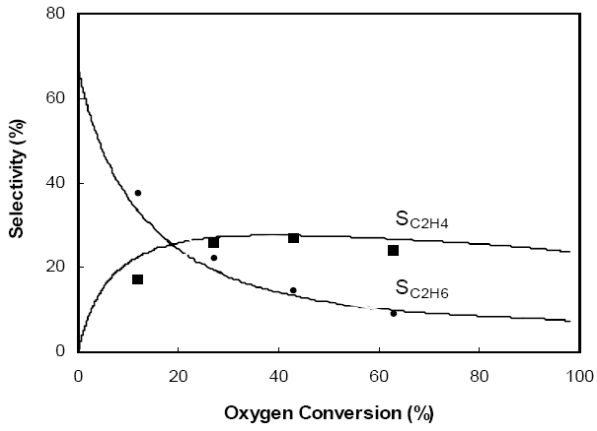

Figure 8. Comparison between modeling results and experimental data. T = 1078 K, eq = 4, P = 4 bar, t_{ave}= 0.5 sec (Isothermal cond.)

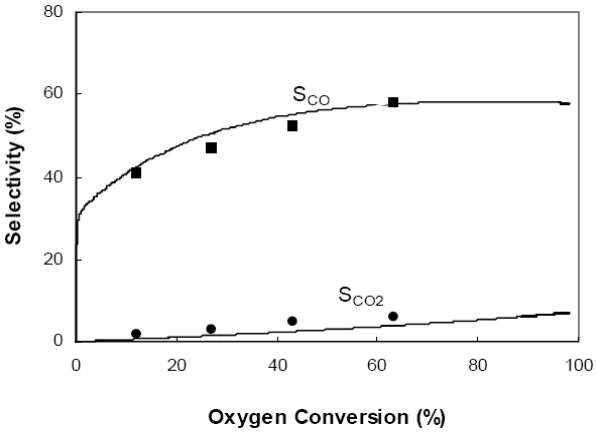

Figure 9. Comparison between modeling results and experimental data.T = 1078 K, eq = 4, P = 4 bar, t_{ave}= 0.5 sec (Isothermal cond.)

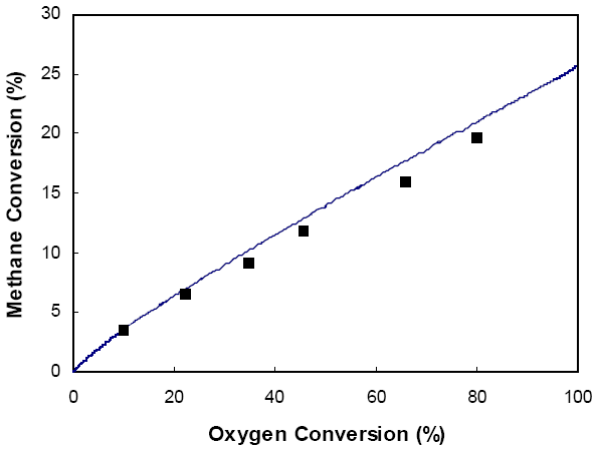

Figure 10. Comparison between modeling results and experimental data's. T = 1078 K, eq = 4, P = 4 bar, t_{ave}= 0.5 sec (Isothermal cond.)

b. The performance of the System under Adiabatic Conditions

Reduction in the ratio of methane to oxygen, results in an increased reaction rate. The amount of methane conversion (Figure 11), decreases the maximum selectivity of the desired products, and increases the maximum selectivity of undesired products. Also by decreasing the ratio of methane to oxygen in the feed, the maximum adiabatic temperature of the system and the maximum selectivity of acetylene increase (Figure 12). Considering that production of acetylene requires a high temperature, the latter results appear reasonable.

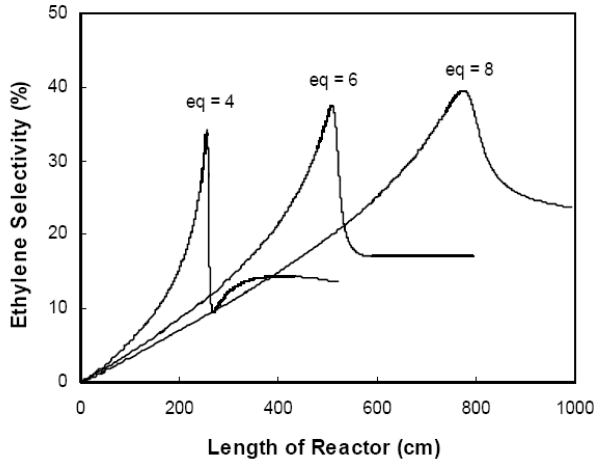

Figure 11. Effect of eq on the rate and ethylene selectivity. P_0 = 4 bar, T_0 = 975 K, $F_{CH4,0}$ = 0.84 mol/sec (Adiabatic cond.)

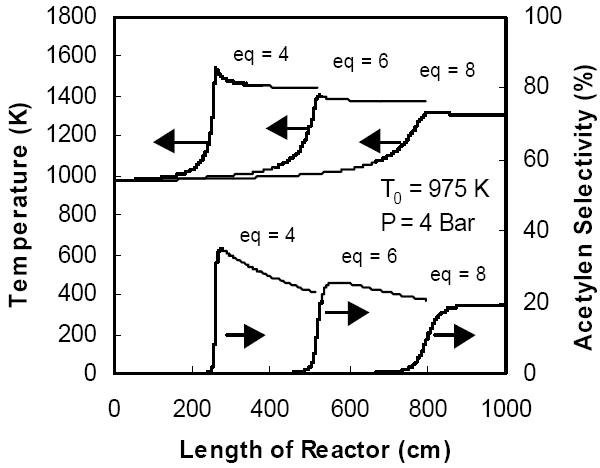

Figure 12. Effect of eq on the temperature profile and acetylene selectivity. P_0 = 4 bar, T_0 = 975 K, $F_{CH4,0}$ = 0.84 mol/sec (Adiabatic cond.)

On the other hand, increasing the initial temperature of the system has no remarkable effect on the methane conversion and product selectivity, and only increases the reaction rate. The maximum adiabatic temperature of the system will not change, too (Figure 13).

Increasing the total pressure of the system causes the rate and conversion of methane to increase (Figure 14). Further, by increasing the pressure, the reactions producing desired products will be favored, hence the selectivities of desired products will increase and

those of undesired ones will decrease, though these variations are not pronounced. Also by increasing the pressure, the maximum adiabatic temperature of the system and the maximum selectivity of acetylene decrease slightly. This behavior is due to decreasing selectivities of undesired products at higher pressure taking place, releasing a considerable amount of heat.

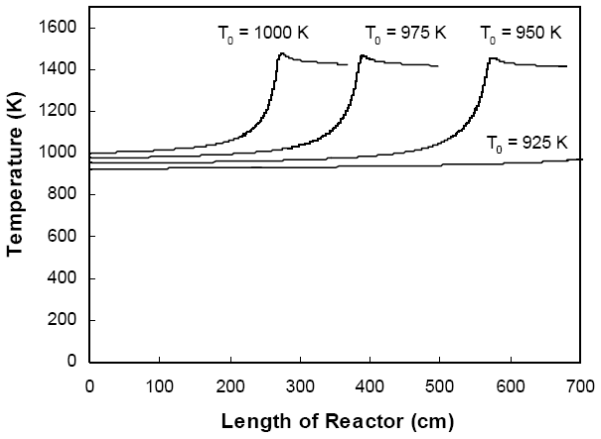

Figure 13. Effect of inlet temperature on the tem-perature gradient along the reactor. P_0 = 4 bar, eq = 5 , $F_{CH4,0}$ = 0.84 mol/sec (Adiabatic cond.)

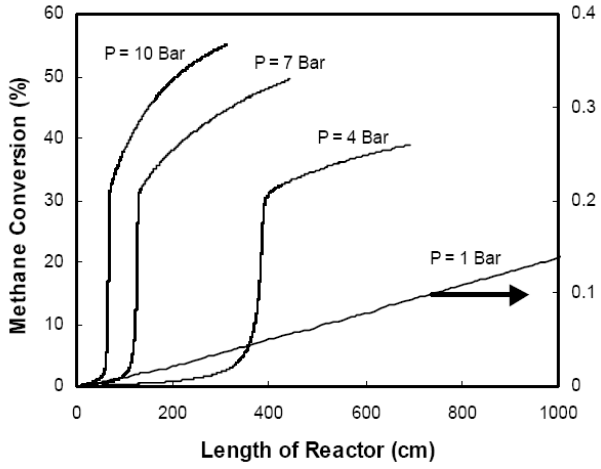

Figure 14. Effect of Total pressure on the rate and amount of methane conversion. T_0 = 975 K, eq = 5, t_{ave} = 0.75 sec , $F_{CH4,0}$ = 0.84 mol/sec (Adiabatic state)

Figure 15 displays variations in the molar rate of the two-carbon molecular hydrocarbons along the reactor. Comparison of results of this figure with those of Figure 2 shows that under adiabatic operating conditions, the molar ratio of acetylene to ethylene increases remarkably due to the temperature increase of the system.

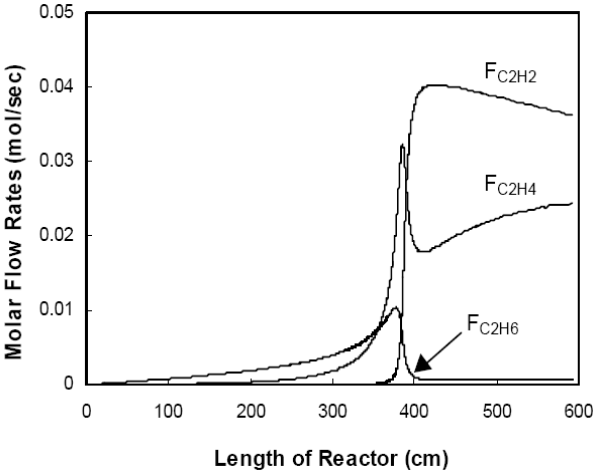

Figure 15. Variation of molar flow rate of C2 compounds along the reactor. T_0 = 975 K, eq = 5, t_{ave} = 0.75 sec , P = 4 bar (Adiabatic state)

Investigation of the heat of reaction shows that by increasing the ratio of oxygen to methane in the feed, the maximum enthalpy change of the whole system as well as the amount of released heat per reacted mol of methane increase (Figure 16). Furthermore, by increasing the total pressure of the system, the maximum enthalpy change of the total system is enhanced and a relative decrease in the released heat per reacted methane molecules occurs.

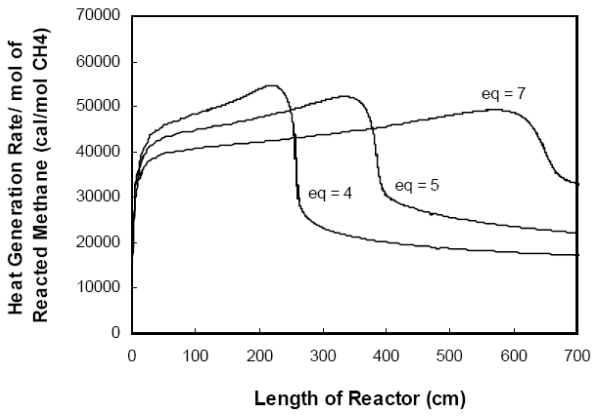

Figure 16. Effect of eq on the released heat per reacted mol of methane. T_0 = 975 K, P= 4 bar, $F_{CH4,0}$ = 0.84 mol/sec (Adiabatic state)

Although the pressure drop along the empty tubular reactor is negligible, in order to attain higher accuracy in the calculations, the pressure variation due to losses has been taken into account in determination of the species molar rates. Variations of the pressure and temperature of the system along the reactor are shown in Figure 17 under the adiabatic condition. Note that the pressure drop is negligible, whereas the temperature variation of the system is very profound.

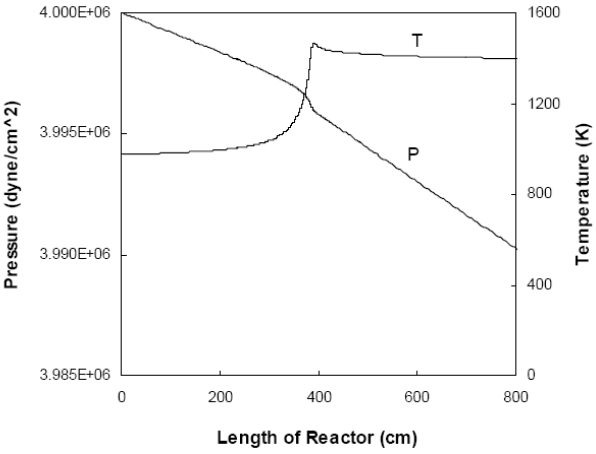

Figure 17. Variation of temperature and pressure along the reactor. T_0 = 975 K, eq = 5, t_{ave} = 0.75 sec , P_0 = 4 bar (Adiabatic state)

Conclusions

A reactor-kinetic model has been used to simulate the gas phase oxidative coupling of methane, under both isothermal and adiabatic operating conditions. The reactions of the gas-phase OCM process are highly exothermic, resulting in remarkable changes in the temperature of the system. Increase in temperature during the reaction for the adiabatic state will result in major changes in the distribution of products as compared to the constant-temperature state. Due to remarkable increase of temperature under adiabatic conditions, the reaction rates and product selectivity will be severely affected. Increase in pressure of the system causes an increase in selectivity of desired products and increase in conversion of methane; in this case, the efficiency of the gas-phase process is comparable to that of the catalytic process. Increasing the ratio of methane to the inlet oxygen causes an increase in the selectivity of the desired products and a decrease in the amount of methane conversion. On the other hand, an increase in the inlet temperature of the reactants under adiabatic conditions causes an increase in the rates of the reactions and has no considerable effect on other parameters of the system such as product selectivity and maximum adiabatic temperature.

Nomenclature

A	inner area of reactor (cm^2)
A_i	pre-exponential factor of rate constant (sec^{-1} or cm^2 mol^{-1} sec^{-1} or cm6 mol^{-2} sec^{-1})
C_{Pk}	molar heat capacity of species k at constant pressure (cal/mol. K)
C_{T0}	initial total concentration of gas phase (mol/cm^3)
D	inner diameter of reactor (cm)
eq	ratio of methane to oxygen
E_{act}	activation energy (cal/mol)
f	friction factor
F_k	molar flow rate of species k (mol/sec)
F_T	total molar flow rate (mol/s)
G	mass velocity (g/cm^2.sec)
H	step size
H_k^0	standard molar enthalpy of species k (cal/mol)
H_k	molar enthalpy of species k (cal/mol)
i	number of reaction
I	total number of reaction
J	order of BDF (Backward Difference Formulas)
k	symbol of each chemical species
k_{fi}	forward rate constant for reaction i
k_{ri}	backward rate constant for reaction I
K	total number of chemical species
L	total length of tube (cm)
n_c	number of carbon atoms
P	total pressure (dyn/cm^2)
P_0	let pressure (dyn/cm^2)

P_{atm} atmospheric pressure (dyn/cm^2)
r_i rate of reaction i
r_{ik} production rate of species k at reaction i
R general constant of gases (cal/mol. K)
S_k selectivity of species k
S^0_k standard molar entropy of species k (cal/mol. K)
t time of reaction
T absolute temperature (K)
T_0 inlet temperature (K)
t_{ave} average residence time (sec)
U linear speed (cm/sec)
V system volume (cm^3)
W average molecular weight (g/mol)
X_k conversion of species k
x differential equation formed for each species and energy
y length dimension of reactor

Greek Symbols

β non-linear function of rate constant
ν'_k stoichiometric coefficient of forward reaction of species k in reaction i
ν''_k stoichiometric coefficient of backward reaction of species k in reaction i
ρ density of bulk gas (g/cm^3)
ω_k production rate of species k

References

1. Badakhshan, A., MSc program in energy and the environment: air pollution and its impact on energy development, Vol. II, 1997-1998, Calgary University.
2. Billaud, F.G.; Ueret, C. P. and Baronnet, F., Ind. Eng. Chem. Res., 1992, 31, 2748-2753.
3. Asami, K.; Shikada, T.; Fujimoto, K. and Tominaga, H. O., Ind. Eng. Chem. Res., 1987, 26, 2348-2353.
4. Zanthoff, H. and Baerns, M., Ind. Eng. Chem. Res., 1990, 29, 2-10.
5. Chen, Q.; Hoebink, J. H. B. J. and Marin, G. B. ,Ind. Eng. Chem. Res., 1991, 30, 2088-2098.
6. Chen, Q.; Couwenberg, P.M. and Marin, G.B., AICHE J., March 1994, Vol. 40, No. 3, 521-535.
7. Tjatjopoulos, G.L. and Vasalos, I.A., Appl. Catal., 1992, 88, 213-230.
8. Geerts, J. W. M. H.;Chen, Q.;Van Kastern, J. M. N. and Wiele, K. V. D. ,Catal. Today, 1990, 6, 519-526.
9. Chen, Q.;Couwenberg, P.M. and Marin, G. B., Catal. Today, 1994, 21, 309-319.
10. Serauskas, B.;Hampson, R.F.; Tsang, W.; Frenklack, M., GRI-Mech: Natural Gas Combustion Mechanism., Monteral Poly-tech. Gas research Institute Report, 1996, (www.me.berkeley.edu/gri_mech/).
11. Tsang, W. and Hampson, R. F., J. Phys. Chem. Ref. Data, 1986, 15, 1087.
12. Mohammadi, A. R., M. S. thesis, Dep. Chem. Eng., Sharif University of Tech., Iran, Sep. 2000.
13. Ludwig,E.E., Applied Process Design for Chemical and Petrochemical Plants., Gulf Publishing Co., second edition, 1997.
14. Fogler,H.S., *Elements of Chemical Reaction Engineering.*, Prentice-Hall International , Third Edition, New Jersey ,1999.